Glioblastoma-targeted, local and sustained drug delivery system based on an unconventional lipid nanocapsule hydrogel

Claire Gazaille, Elia Bozzato, Adélie Mellinger, Marion Sicot, Umer Farooq, Patrick Saulnier, Joël Eyer, Véronique Préat, Nicolas Bertrand, Guillaume Bastiat

Targeted, local and sustained drug delivery system based on lipid nanocapsule-based hydrogel for the treatment of glioblastoma

Claire Gazaille[a], Elia Bozzato[b], Neda Madadian-Bozorg[c], Adélie Mellinger[a], Marion Sicot[a], Umer Farooq[a], Patrick Saulnier[a], Joël Eyer[a], Véronique Préat[b], Nicolas Bertrand[c] and Guillaume Bastiat[a,*]

a Univ Angers, Inserm, CNRS, MINT, SFR ICAT, F-49000 Angers, France
b UCLouvain, Louvain Drug Research Institute, Advanced Drug Delivery and Biomaterials, Brussels, Belgium
c Univ Laval, Faculty of Pharmacy, CHU Quebec Research Center, Québec, QC, Canada
* Corresponding author: guillaume.bastiat@univ-angers.fr

PUBLISHED IN BIOMATERIALS ADVANCES

https://doi.org/10.1016/j.bioadv.2023.213549

Abstract

The objective of this work was to develop an implantable therapeutic hydrogel that will ensure continuity in treatment between surgery and radiochemotherapy for patients with glioblastoma (GBM). A hydrogel of self-associated gemcitabine-loaded lipid nanocapsules (LNC) has shown therapeutic efficacy *in vivo* in murine GBM resection models. To improve the targeting of GBM cells, the NFL-TBS.40-63 peptide (NFL), was associated with LNC. The LNC-based hydrogels were formulated with the NFL. The peptide was totally and instantaneously adsorbed at the LNC surface, without modifying the hydrogel mechanical properties, and remained adsorbed to the LNC surface after the hydrogel dissolution. *In vitro* studies on GBM cell lines showed a faster internalization of the LNC and enhanced cytotoxicity, in the presence of NFL. Finally, *in vivo* studies in a murine GBM resection model proved that the gemcitabine-loaded LNC with adsorbed NFL could target the non-resected GBM cells and significantly delayed or even inhibited the apparition of recurrences.

Keywords

Lipid nanocapsules, Hydrogel, Sustained release, Targeting, Glioblastoma

Introduction

Glioblastoma (GBM) is the highest-grade glioma tumor according to the World Health Organization and the most common primary tumor of the central nervous system in adults [1]. It is often diagnosed in old and middle-aged patients (average age at diagnosis is 65 years old), with an incidence of 3.23 cases per 100,000 individuals. Recent data from the Central Brain Tumor Registry of the United States (CBTRUS) reports that the median survival for all patients with GBM is 8 months regardless of treatment, with a five-year survival rate of 7.2% [2,3]. The aggressiveness of GBM is due to high infiltration and rapid proliferation of tumor cells, and to important intra- and inter-tumor heterogeneity leading to global chemoresistance [4]. The standard of care for GBM includes neurosurgery with maximal tumor resection, followed by Stupp's protocol: radiotherapy and concomitant oral administration of temozolomide (TMZ), a non-specific alkylating agent [5]. Among all concomitant and/or adjuvant approved therapeutic agents (lomustine and carmustine in the 70's), TMZ led to the best therapeutic efficacy in the clinic with a median survival of 14.6 months, and a 5-year survival rate of 10%, again confirmed by a recent meta-analysis [6]. Despite this prolonged survival, this gold standard is not curative, and does not allow the elimination of all GBM cells: most fatal tumor recurrences occur at the periphery of the primary tumor resection [7]. This protocol has not evolved since 2005, and it is now urgent to improve the management of patients with GBM with new therapeutic alternatives.

Two strategies stand out among all preclinical studies dealing with this pathology. The first is to improve the passage of therapeutic agents through the blood-brain barrier (BBB) using specific nanodrug delivery system, alone [8], or in combination with physical methods that transiently increase the barrier's permeability [9,10]. The second approach is the local delivery of drugs directly to the tumor or in the GBM resection cavity [11-13]. In preclinical models of brain cancer, a recent meta-analysis highlighted the increased efficacy of local administration over systemic treatment, irrespective of the drug, the drug delivery system or the *in vivo* preclinical model [14]. Local treatment is particularly attractive since resection of the primary tumor is part of the clinical standard procedure. In 1998, the US Food and Drug Administration approved the Gliadel® wafers as the first post-operative implant against newly diagnosed or recurrent GBM. These wafers are polymer microspheres (composed of Polifeprosan 20) loaded with the alkylating agent carmustine, and compressed into solid discs [15,16]. A retrospective analysis on patients that had received a first diagnosis of GBM between 1997 to 2006, showed that the addition of Gliadel® to Stupp's protocol increased median survival in comparison to Stupp's protocol alone, *i.e.* 20.7 months (33 patients) *vs* 14.7 months (45 patients), respectively [17]. Even though the efficacy of the Gliadel® wafers combined with Stupp's protocol was proven by other clinical trials involving newly diagnosed GBM patients [18], risk-to-benefit ratio and high costs still limit its clinical use [19,20]. The rigidity of the wafers contributes to several severe side effects after implantation: seizures, intracranial hypertension, meningitis, cerebral edema, and poor wound healing [19,21]. Moreover, these adverse effects are enhanced by the slow degradation of the polymer wafers: implant remnants were observed during autopsies and reoperations, as long as 232 days post-implantation (Food and Drug Administration. Reference ID 3358686. Available at: https://www.fda.gov/). In addition, some limits were observed *in vivo* such as a fast release of carmustine (about 75% of the drug released in the first week after implantation) [22], a limited

diffusion in the tissue surrounding the resection cavity, and non-specificity of the drug toward residual GBM cells [21,23,24]. Hence, local therapy of GBM could benefit from improvements in the drug delivery system, as well as the therapeutic payload.

To overcome the limits in stiffness and biodegradability of current implants, we recently developed polymer-free hydrogels composed of lipid nanocapsules (LNC). In this system, the hydrogel scaffold results from the association of concentrated suspensions of LNC, decorated at the oil/water interface with amphiphilic crosslinking agents. Examples of cross-linking agents include cytotoxic 4-*N*-lauroyl gemcitabine (GemC12), and non-cytotoxic 4-*N*-palmitoyl cytidine (CytC16). The H-bond interactions between the pyrimidine moieties lead to the crosslinking between nanoparticles [25,26]. A key advantage over other nanoparticle-loaded systems is that the hydrogel fully degrades by releasing Gem-C12- or CytC16-loaded LNC, without residual polymers or crosslinking agents [27]. Such a system was successfully tested in tumor murine models i) to delay the appearance of mediastinal metastases during lung cancer progression after a subcutaneous administration [28], and ii) to delay GBM recurrence, filling the resection cavity after surgery. In an orthotopic murine model of surgically resected U-87 MG GBM, the administration of hydrogels prepared with GemC12-loaded LNC significantly delayed the apparition of fatal recurrences compared to local administration of equivalent doses of gemcitabine solution: median survivals of 62 *vs.* 36 days, respectively [29]. Unlike a liquid, implantation of the hydrogel in the resection cavity sustains the exposure of residual GBM cells to the drug. This increased antitumor activity was also observed in a rat model of orthotopic GBM resection [30]. In addition, this original drug delivery platform can be used to combine drugs with different mechanisms of action and achieve improved *in vitro* antitumor efficacy in GBM cell lines [31]. Finally, short- and long-term studies in healthy mice suggested that hydrogels composed of GemC12-loaded LNC were well-tolerated, for 2 and 6 months after implantation [29,32].

LNC-based hydrogels have demonstrated their potential for the local treatment of GBM. However, the LNC released from the hydrogel do not have inherent tropism for GBM cells. As with Gliadel® wafers, this lack of specificity could result in off-target toxicities. Hence, we propose to decorate the surface of LNC with a targeting ligand, to explore the potential of combining active targeting with local, sustained administration. In the literature, suspensions of ligand-decorated nanoparticles are commonly used to target GBM cells, GBM cancer stem cells, tumor-associated myeloid cells and the extracellular matrix [33]. Previously, we used the NFL-TBS.40-63 peptide (NFL) to improve the *in vitro* cellular uptake of LNC suspensions by GL261 cells, compared to LNC without NFL [34,35]. The NFL peptide corresponds to the tubulin-binding site on the light neurofilament subunit and it selectively enters various GBM cell lines (9L, F98, GL261, T98G and U-87 MG) *in vitro* [34,36-39]. Due to its cationic nature, the peptide partially adsorbs to the surface of LNC in suspension, by simple incubation at room temperature. Treatment of GL261 cells with suspensions of NFL-functionalized LNC containing paclitaxel resulted in decreased *in vitro* proliferation, and slightly reduced tumor progression compared to non-functionalized LNC loaded with paclitaxel [34]. In this study, the mice bearing orthotopic GL261 cell xenografts received one single intra-tumor injection of paclitaxel-loaded LNC.

Our hypothesis is that sustained delivery of LNC could enhance the targeting efficacy of NFL. Combining the NFL and the LNC-based hydrogel required modifying the gel preparation method and ensuring that the adsorption of the peptide did not disrupt the mechanical and releasing properties of the hydrogel.

We then evaluated the *in vitro* efficacy of the LNC released from the hydrogels, both in terms of specific targeting to GBM cells and improved cytotoxicity. Finally, using a murine model of GBM resection, the *in vivo* efficacy of the LNC-based hydrogels has been determined, also in terms of brain distribution and improved survival.

Materials and Methods

Materials

Kolliphor® HS15 (Kol) was purchased from BASF (Ludwigshafen, Germany). Labrafac® WL 1349 (Lab) was provided by Gattefossé S.A. (Saint-Priest, France). NaCl was purchased from Prolabo (Fontenay-sous-bois, France). Deionized water (Water) was obtained from a Milli-Q plus® system (Millipore, Bilerica, United States). The biotinylated NFL-TBS.40–63 peptide (NFL) was synthesized by the PolyPeptide group (Strasbourg, France). Span® 80 (Span80), sodium cholesteryl sulfate (SChol), and didodecyldimethylammonium bromide (DDAB) were supplied by Sigma-Aldrich (Saint-Quentin-Fallavier, France). GemC12 and CytC16 were synthesized as already reported [26]. Acetone, 1,1'-dioctadecyl-3,3,3',3'-tetramethylindocarbocyanine perchlorate (DiI), 1,1'-dioctadecyl-3,3,3',3'-tetramethylindodicarbocyanine 4-chlorobenzenesulfonate (DiD) and 4-(p-dihexadecylaminostyryl)-N-methylpyridinium iodide (DiA) were purchased from Thermo Fisher Scientific (Illkirch-Graffenstaden, France).

LNC suspension formulation and incubation with NFL

The LNC formulation was an already reported and patented emulsification method: a phase-inversion process from oil-in-water emulsion at low temperature to water-in-oil emulsion at high temperature [26,40]. The quantities of oil phase (Lab), aqueous phase (Water and NaCl) and surfactants (Kol, Span80 w/ or w/o SChol or DDAB) were precisely weighed for each formulation (See supplementary Table S1 for the compositions). To summarize, anionic (with SChol), cationic (with DDAB) and neutral (without SChol nor DDAB) LNC have been made with a Span80 weight composition of 27% (w/w_{Lab}) and neutral LNC have been made with additional Span80 compositions of 0 and 54% (w/w_{Lab}). Briefly, 3 temperature cycles, from 40 to 90°C, were performed under magnetic stirring. During the last cooling step, 1.833 mL of cold Water (4°C) was added at the temperature of the phase inversion zone (between 50 and 75°C depending on the formulation), always under magnetic stirring, leading to the LNC suspension. Then, the LNC suspensions were cooled under magnetic stirring for 5 min until reaching room temperature. For all the formulations, the final LNC concentration in the suspension is constant: 428.6 mg/mL and the LNC suspensions were stored at 4°C. After their characterizations, 350 µL of the LNC in suspension and 150 µL of NFL at 5, 10 or 15 mg/mL solubilized in Water were mixed for 30 sec (vortex) or 1 h (magnetic stirring) at room temperature. The final concentration of LNC in suspension was 300 mg/mL while the final concentrations of NFL peptide were 1.5, 3 or 4.5 mg/mL.

LNC-based hydrogel formulation with or without NFL

The LNC-based hydrogel formulation was based on the same phase-inversion process [25,26,29-32]. The quantities of oil phase (Lab), aqueous phase (Water and NaCl) and surfactants (Kol, Span80, w/ or w/o SChol or DDAB) are the same that for LNC suspension formulation (see supplementary Table S1) and GemC12 or CytC16 were added to obtain the hydrogel. All ingredients were precisely weighed for

each formulation. To summarize, neutral LNC-based hydrogel (Span80 27% (w/w_{Lab})) were done with GemC12 7.5% (w/w_{Lab}) or CytC16 2.5 or 5% (w/w_{Lab}); anionic LNC-based hydrogel (Span80 27% (w/w_{Lab})) were done with GemC12 7.5% (w/w_{Lab}) or CytC16 2.5 or 5% (w/w_{Lab}); and cationic LNC-based hydrogel (Span80 27% (w/w_{Lab})) were done with CytC16 at 5% (w/w_{Lab}). Briefly, GemC12 or CytC16 were first solubilized in a mixture of Lab, Span80 and acetone. Acetone was evaporated before the addition of Kol, NaCl, and Water. The rest of the formulation process was the same as for the LNC formulation for the temperature cycles and the addition of cold Water at the phase inversion zone during the third cooling step. When the formulation reached 37°C, 2.5 mL of Water or NFL at 5, 10 or 15 mg/mL (dissolved in Water) were added under magnetic stirring and syringes were filled with the suspensions before the increase in viscosity, already observed with the LNC-based hydrogels, even without NFL [25,26]. Syringes were stored at 4°C and the gelation process was achieved after 24 h. LNC-based hydrogels were also designed with fluorescent dyes loaded in the LNC. For this purpose, DiA or DiI or DiD were first solubilized in Lab and Span80 at the concentration of 0.4% (w/w_{Lab}) before to add GemC12 or CytC16. The final concentration of LNC in the hydrogels was 300 mg/mL while the final concentrations of NFL were 0, 1.5, 3 or 4.5 mg/mL.

Pictures of LNC-based hydrogels by confocal microscopy

LNC-based hydrogels loaded with DiI or DiA 0.4% (w/w_{Lab}), before or after dissolution in Water, were analyzed by confocal microscopy using a Leica TCS SP8 AOBS confocal laser scanning microscope (Leica Microsystems, Germany) equipped with an HC PL APOCS2 63X/ON 1.4 (Oil immersion) objective. DiI was excited with the 561 nm line of a diode laser (20 mW) while DiA was excited with the 488 nm line of an argon-ion laser (40 mW). The fluorescence emission was collected using a gateable GaAsP hybrid detector (between 565 and 624 nm and between 492 and 627 nm, for DiI and DiA, respectively). The scan rate for the acquisition of micrographs was 400 Hz, and data were stored as 1024 pixel 8-bit.

Size distribution and zeta potential measurements

The size distribution: hydrodynamic diameter (Z-ave) and polydispersity index (PdI), and zeta potential (ZP) of both LNC in suspensions and LNC-based hydrogels (before the completion of gelation) were measured using a Zetasizer® Nano ZS (Malvern Panalytical Ltd., United Kingdom). The quasi-elastic light scattering instrument is equipped with a 4-mW Helium–Neon laser with an output wavelength of 633 nm and a scattering angle fixed at 173°. The correlation functions were fitted using an exponential fit (Cumulant approach) for the Z-ave and PdI determinations. The Smoluchowski approximation was used to determine the electrophoretic mobility required for ZP determination. All the measurements were performed at 25°C at a LNC suspension concentration of 5 mg/mL (dilution in Water).

Rheological properties

The viscoelastic properties of the LNC-based hydrogels after completed gelation, extruded from syringes without needle, were measured at 25°C using a Kinexus® rheometer (Malvern Panalytical Ltd, United Kingdom) with a cone plate geometry (diameter: 40 mm, angle: 2°). Oscillatory strain sweeps at a constant frequency of 1 Hz were performed to determine the linear regimen characterized by the constant dynamic moduli (elastic modulus: G’ and viscous modulus: G”), independent of the strain amplitude. In this regimen (0.1% constant oscillatory strain amplitude), G’ and G” were measured as a function of oscillatory frequency (from 0.1 to 10 Hz) to determine the viscoelastic properties. In addition, the flow behaviors of the LNC-based hydrogels were evaluated at 25°C measuring the

viscosity variation as a function of controlled shear rates ranging from 0.1 to 100 s^{-1}. Two cycles with successive increasing and decreasing shear rates were performed to characterize the thixotropic behavior.

UPLC quantification of free NFL in the LNC suspensions or in the LNC-based hydrogels

The free NFL concentrations in the LNC-based hydrogels or the LNC suspensions were measured using an Acquity® H-Class Bio UPLC apparatus (Waters, France) as already reported [40]. Briefly, after the LNC-based hydrogel dissolution in Water or the use of LNC suspensions at the same concentration, the LNC suspensions with adsorbed or free NFL were filtered through 0.22 µm. The separation between the NFL-adsorbed LNC and free NFL was carried out using an Acquity UPLC Protein BEH SEC column (200 Å, 1.7 µm, 4.6 mm × 300 mm), with an Acquity UPLC® Protein BEH SEC Guard Column (200 Å, 1.7 µm, 4.6 mm × 30 mm, 10 K - 500 K), at room temperature under isocratic conditions (mobile phase: NaCl at 0.1 M in Water). The flow rate was maintained at 0.3 mL/min, the injection volume was 10 µL, and the detection wavelength of the UV detector was set to 220 nm. Retention time for NFL-adsorbed LNC and free NFL were 3.4 and 7.7 min, respectively. A calibration curve from solutions of standards (NFL from 0 to 500 µg/mL in Water) was used to quantify the free NFL concentrations (determination coefficient: 0.997).

Release profiles of GemC12, CytC16, NFL and LNC from LNC-based hydrogels and HPLC quantification

The release profiles were obtained over a period of up to two weeks of incubation in Dulbecco's phosphate buffered saline (DPBS 1X) (Thermo Fisher Scientific, France). Fifty mg of LNC-based hydrogels were weighed at the bottom of a 200 µL PCR tube (VWR International, United States), filled with DPBS 1X, and inverted in a 2 mL microtube (STARLAB GmbH, Germany) with a screwable cap containing a total of 1,500 µL of DPBS 1X and a 2 x 7 mm magnetic stir-bar. The tubes were incubated at 37°C and continuously stirred at 50 rpm. At specified time intervals, 300 µL of sample were taken and replaced with an equal volume of fresh DPBS 1X. At the end of the incubation period (14 days), the residual gel was properly dissolved in the DPBS 1X and analyzed to obtain the total quantity of analytes encapsulated in the gel. Each sample was split to analyze GemC12/CytC16, and the NFL separately by high-performance liquid chromatography (HPLC) analysis.

The LNC release from the hydrogel was evaluated by fluorescence measurements (excitation and emission wavelengths of 488 and 610 nm, respectively, using FluoroMax®-4 spectrophotometer (HORIBA Jobin Yvon Inc., United States). The proportion of released LNC was calculated using a calibration curve of DiA-loaded LNC-based hydrogel dissolved in DPBS 1X (determination coefficient: 0.998 – 0.999).

NFL, GemC12 and CytC16 were quantified on an Agilent 1260 infinity II HPLC equipped with a diode-array detector, using a Poroshell Infinity Lab 120 EC-C18 column (100 x 4.6 mm, 4 µm, Agilent technologies, United States). The temperature of the autosampler was controlled to 4°C to prevent sample degradation, and the temperature of the column oven was set to 40°C.

The content of GemC12 and CytC16 was determined without extraction, using 20 µL of the release sample. The mobile phase consisted of Water (TFA 0.1% (*v/v*)) and methanol (HPLC grade). Separation was conducted at a flow rate of 1 mL/min, using a gradient: 0 → 2 min: 30% Water; 2 → 10 min: linear increase until 100% methanol; 10 → 12 min: 100% methanol; 12 → 15 min: return to 30% Water. Under these conditions, GemC12 had a retention time of 6.87 min, and CytC16 of 9.87 min. Detection was carried at 250 nm. A calibration curve from solutions of standards in 25 % (*v/v*) methanol in PBS was

used, with a concentration range of 10 – 120 µg/mL (determination coefficient for GemC12 and CytC16: 0.998 - 0.999).
For total NFL quantification, 75 µL of the release sample were spiked with 10 µL of internal standard (vancomycin at 0.5 mg/mL in methanol). Twenty µL of a 5mg/mL tetraethylammonium fluoride hydrate solution in methanol were added to desorb NFL from sodium cholesteryl sulfate. Liquid-liquid extraction was done by adding 32.5 µL of methanol and 31.2 µL of chloroform to the aqueous sample. The biphasic solution was vortexed and an additional 37.6 µL of chloroform and 12.5 µL of 0.5 M acetate buffer at pH 4.5 were added. After vortexing, the samples were centrifuged at 9,720 g for 5 min. Fifty µL of the upper aqueous phase were collected and transferred to a new tube, 80 µL of ultrapure Water were added and mixed, before injecting 100 µL in the HPLC. Using the same mobile phase as above, separation was conducted at a flow rate of 1 mL/min, using a gradient: 0 → 1 min: 77% Water; 1 → 2.5 min: linear gradient until 47% methanol; 2.5 → 5.5 min: 47% methanol; 5.5 → 7.5 min: linear gradient until 100% methanol, and 7.5 → 8.5 min: linear gradient until 77% Water, then 5 minutes of equilibration. NFL was quantified at 210 nm, using the ratio of NFL peak (retention time of 4.37 min) over the peak of the internal standard (retention time of 2.39 min). The calibration curve was obtained by extracting NFL solutions in PBS as described above (concentration range 0.8 – 4 µg/mL) (determination coefficient: 0.994). To mimic the sample matrix, sodium cholesteryl sulfate, and LNC in methanol (18 µL) were added to standards and the volume of methanol used in the extraction was adjusted to 14.5 µL.

Cell culture

U-87 MG human glioma cell line (ATTC, United States) was cultured in Eagle's Minimum Essential Medium (EMEM) (ATTC, United States) supplemented with 10% Fetal Bovine Serum, and 1% of 10000 U/mL Penicillin G and 10,000 µg/mL Streptomycin (Biowest, France). GL261 and F98 human glioma cell lines (ATTC, United States) were cultured in high glucose Dulbecco's Minimum Essential Medium (DMEM) (Sigma-Aldrich, France) supplemented with 10% Fetal Bovine Serum, and 1% of 10000 U/mL Penicillin G and 10,000 µg/mL Streptomycin. NHA human astrocyte cell line (ATTC, United States) was cultured in Astrocyte Growth Medium BulletKit medium (Lonza, France) supplemented with ACM SingleQuot™ kit (Lonza, France).

Internalization

LNC-based hydrogels with CytC16 2.5 or 5% (w/w_{Lab}), with or without NFL and loaded with DiA or DiI 0.4% (w/w_{Lab}) were first dissolved to reach a LNC suspension concentration of 10 mg/mL (dilution in Water). Then the LNC suspensions were dissolved in cell culture media at a LNC suspension concentration of 0.6 mg/mL. U-87 MG, GL261 and F98 cells were seeded in a 12-well plate at 8×10^4 cells per well for 48 h at 37°C / 5% CO_2. NHA cells were seeded in a 12-well plate at 6×10^4 cells per well for 48 h at 37°C / 5% CO_2. After 3 or 6 h incubation, cells were washed once with DPBS 1X and cell culture medium without LNC was added once again. Cells were dissociated with trypsin-EDTA 1X (Biowest, France) at 37°C for 5 min, then centrifuged (140g, 5 min) and suspended in DPBS 1X. This washing step was repeated 4 times. Trypan blue (0.012% (*v/v*)) (Thermo Ficher Scientific, France) was added to the cells before flow cytometry analysis using a MACSQuant® analyzer 10 (Miltenyi Biothec, Germany) with 5,000 to 20,000 cells analyzed per sample (excitation and emission wavelengths of 488 and 585/40 nm, respectively). For confocal microscopy analysis, the cells were seeded on glass slides. After the incubation with LNC suspensions, the cells were washed three times 5 min with DPBS 1X and

fixed with PFA at 4% (*v/v*) (Sigma-Aldrich, France) for 10 min at room temperature. The cells were washed once again three times 5 min with DPBS 1X and permeabilized with Triton X-100 0.2% (*w/v*) (Biowest, France) for 10 min. The cells were washed once again three times 5 min with DPBS 1X and bovine serum albumin at 5% (*w/v*) (Biowest, France) for 30 min at room temperature. The cells were washed once again three times 5 min with DPBS 1X and incubated with α-Tubulin Monoclonal Antibody Alexa Fluor™ 647 at 2.5 µg/mL (BioLegend, Netherland) during one night at 4°C. The cells were washed once again three times 5 min with DPBS 1X and incubated with DAPI at 3 µM (Sigma-Aldrich, France) for 10 min. Finally, the cells were washed once again three times 5 min with DPBS 1X. Cells were imaged by confocal microscopy (see previous section for the apparatus). DAPI, DiI and Alexa Fluor™ 647 were excited with the 405 nm line of a diode laser (50 mW), the 561 nm line of a diode laser (20 mW) and the 633 nm line of a He/Ne laser (10 mW), respectively. The fluorescence emission was collected using a gateable GaAsP hybrid detector between 408 and 460 nm, between 565 and 624 nm, and between 637 and 755 nm, for DAPI, DiI and Alexa Fluor™ 647, respectively.

Cell viability

LNC-based hydrogels with GemC12 7.5% (w/w_{Lab}), with or without NFL, were first dissolved to reach a LNC suspension concentration of 10 mg/mL (dilution in Water). Then, the LNC suspensions were diluted in the appropriate culture media to have GemC12 equivalent concentrations from 0.003 to 10 µg/mL. U-87 MG, GL261 and F98 cells were seeded in a 12-well plate at 8×10^4 cells per well for 48 h at 37°C / 5% CO_2. NHA cells were seeded in a 12-well plate at 6×10^4 cells per well for 48 h at 37°C / 5% CO_2. After 3 h (U-87 MG and GL261 cells) or 6 h of incubation (F98 and NHA cells) with the LNC suspensions, the cells were washed once with Hank's Balanced Salt Solution 1X (HBSS 1X) and cell culture media without LNC was added once again. After 24 h (GL261, F98 and NHA cells) or 48 h incubation (U-87 MG cells), the cells were washed once with HBSS 1X. Resazurin (diluted in media, final concentration: 0.025 mg/mL) was added to each well, followed by incubation at 37°C / 5% CO_2 for 3.5 h. The reduction of resazurin to resorufin was assessed using a Clariostar microplate reader (BMG Labtech, France) at excitation and emission wavelengths of 560 and 590 nm, respectively. Fluorescence intensity from untreated cells was considered as 100% cell viability ($Fluo^-$), and that from empty wells was considered as 0% cell viability ($Fluo^+$). Cell viability was calculated using the fluorescence intensity of treated cells ($Fluo^t$) with the following equation:

$$\text{Cell viability (\%)} = \frac{\text{Fluo}^{\text{t}} - \text{Fluo}^{+}}{\text{Fluo}^{-} - \text{Fluo}^{+}} \times 100$$

Animal experiments

Six-week-old female NMRI nude mice (Janvier, France) were used for the *in vivo* experiments. Animals had free access to water and food throughout the experiment and their behavior and body weight were constantly monitored. All experiments were performed following the Belgian national regulations guidelines as well as in accordance with EU Directive 2010/63/EU, and were approved by the ethical committee for animal care of the faculty of medicine of the Université catholique de Louvain (2019/ UCL/MD/004).

Mice were anesthetized by intraperitoneal injection of ketamine / xylazine (100 and 13 mg/kg, respectively) and placed on a stereotactic frame to be injected with 4×10^4 U-87 MG cells in the right frontal lobe with a Hamilton syringe as previously described [29,41]. The injection coordinates were 2.1 mm lateral, 0.5 mm posterior from the bregma and 2.5 mm deep from the outer border of the

cranium. The presence of tumors was determined by Magnetic Resonance Imaging (MRI) performed on day 10 after the injection as previously reported [29]. On day 14, the tumor was resected according to the biopsy punch resection model [42]. The resection cavity was filled with 5 µL of a LNC-based hydrogel.

For the biodistribution study, LNC-based hydrogel with CytC16 5 % (w/w_{Lab}) / DiD 0.4% (w/w_{Lab}) / no NFL (n = 2), and the LNC-based hydrogel with CytC16 5 % (w/w_{Lab}) / DiD 0.4% (w/w_{Lab}) / NFL 4.5 mg/mL (n = 2), were administered. The animals were sacrificed on day 20. After 6 days of treatment, no endpoint (body weight loss of more than 20% or body weight loss of 10% plus other clinical signs) was reached. The brains were extracted, frozen in isopentane at -30°C and stored at -80°C before analysis. Frozen brain slices (10 µm with a Leica cryostat) were fixed with cold methanol on Fisherbrand™ Superfrost™ Plus Microscope Slides (Thermo Ficher Scientific, France). The brain slices were washed three times for 5 min with DPBS 1X and incubated with DAPI at 3 µM (Sigma-Aldrich, France) for 10 min. Finally, the brain slices were washed once again three times 5 min with DPBS 1X, before montage with Prolong Diamond (Invitrogen, France). The brain slices were imaged by confocal microscopy (see previous section for the apparatus). DAPI and DiD were excited with the 405 nm line of a diode laser (50 mW) and with the 633 nm line of a He/Ne laser (10 mW), respectively. The fluorescence emission was collected using a gateable GaAsP hybrid detector between 408 and 460 nm and between 637 and 750 nm, for DAPI and DiD, respectively. Images were analyzed using ImageJ (FIJI 1.53t) software (see supplementary method for detailed method).

For the survival study, the doses of administered GemC12 and NFL peptide were 2.0 mg/kg and 0.75 mg/kg, respectively. The LNC-based hydrogel with GemC12 7.5 % (w/w_{Lab}) / no NFL (n=8), and the LNC-based hydrogel with GemC12 7.5 % (w/w_{Lab}) / NFL 4.5 mg/mL (n=8), were administered. The resection cavity was not filled for the untreated group (n=8). When the animals reached the endpoints, mice were sacrificed. The study was not blinded.

Statistical analysis

All the results were expressed as the mean ± standard deviation (SD). Statistical analyses of the results of NFL adsorption, rheological properties, release studies and *in vitro* cell culture studies were performed using the one-way analysis of variance test, followed by the post-hoc Tuckey test for pairwise comparisons. The statistical analysis of the Kaplan-Meyer survival curves was performed through the long-rank (Mantel-Cox) test. Differences were considered statistically significant for $p < 0.05$.

Results and discussion

Anionic LNC drive total and instant adsorption of NFL

LNC-based hydrogels are formulated by thermal cycling, with the final cooling rate influencing the kinetic of hydrogel formations [25,26]. The preparation of hydrogels containing ligand-functionalized LNC requires optimizing peptide adsorption: NFL must be introduced after LNC formation, but before gelation, at a temperature that minimizes its denaturation and/or degradation. We investigated how to adsorb the NFL efficiently and quickly at the surface of LNC. We evaluated the content in Span80, the surface charge of LNC and the concentration of peptide as parameters that could affect the kinetics and extent of NFL adsorption.

First, monodisperse LNC with diameters around 50 nm (Z-ave about 50 nm and PdI < 0.1, supplementary Table S1) were prepared with Span80 at 0, 27 or 54% (w/w_{Lab}), without a crosslinking agent. These suspensions were incubated for 30 sec or 1 h with the NFL, and the proportions of free NFL were quantified by a SEC/UPLC technique [40]. In the absence of Span80, the NFL peptide did not adsorb at the LNC surface, even after one hour of incubation. In fact, we observed that the amount of NFL adsorbed increased proportionally to the Span80 content, both after 30-sec and 1-h incubation (Figure 1A). However, even in the best conditions, the total peptide adsorbed plateaued at ~80%.

To investigate the effect of surface charge, anionic and cationic LNC were prepared (with SChol and DDAB, respectively), and compared to neutral LNC. Addition of charged surfactants did not alter the size distribution of LNC (Z-ave 40 – 50 nm and PdI < 0.1, supplementary Table S1). However, it resulted in modulation of the surface charges, as illustrated by ZP values of -25, 0 and +30 mV for the anionic, neutral and cationic LNC, respectively (Supplementary Table S1). When these nanoparticles were incubated with NFL for 30 s or 1 h, positive charges did not improve adsorption of NFL, compared to reference neutral LNC prepared with Span80 27% (w/w_{Lab}) (Figure 1B). In contrast, addition of the anionic surfactant resulted in total adsorption of NFL, even after very short incubation. This quick and complete surface decoration on anionic LNC was perceived even when the peptide concentration was increased 3-fold (Figure 1C). In comparison, the proportion of peptide adsorbed on neutral LNC remained lower than 80%, irrespective of NFL concentration and incubation time. In conclusion, these results suggest that the adsorption of the NFL depends on the proportion of Span80 and the surface charge of the LNC. With anionic LNC, peptide adsorption occurs very rapidly, and remains complete (< 2% of free NFL) in all ranges of NFL concentration tested.

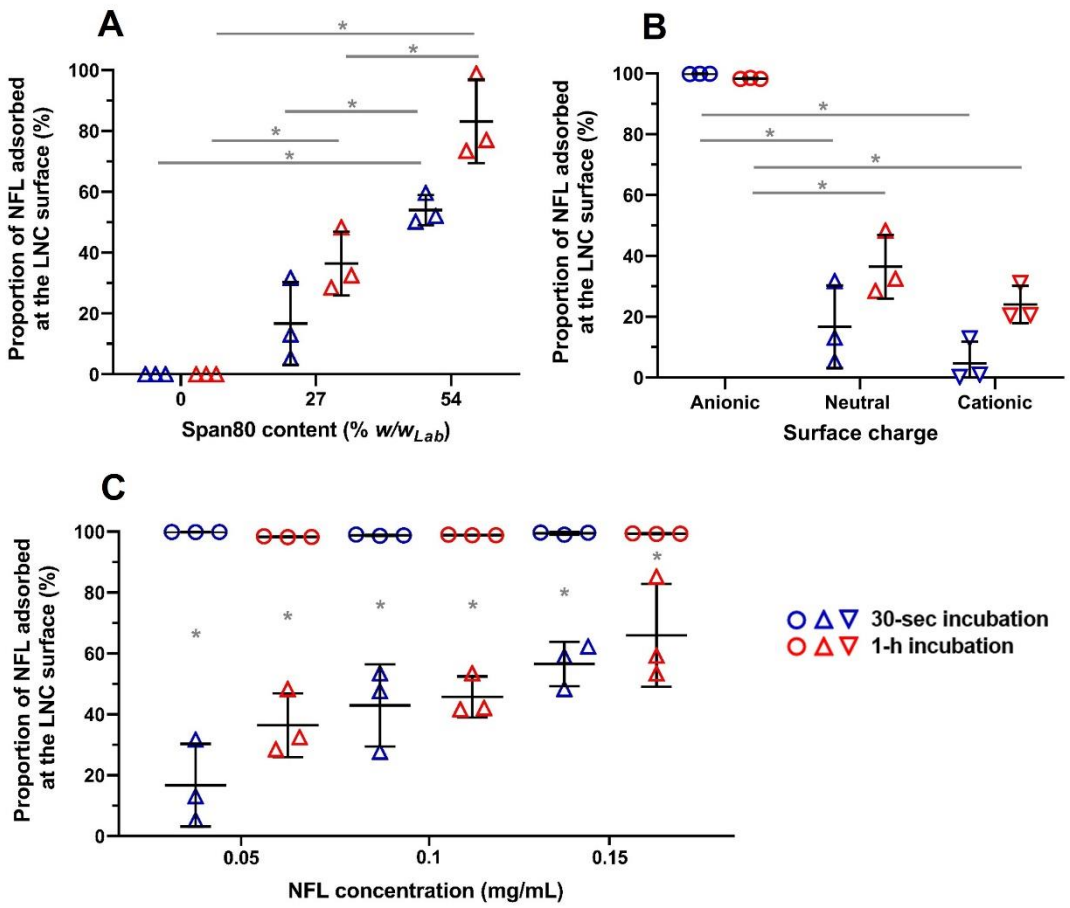

Figure 1. The instant NFL adsorption is mediated by the nature of the LNC surface. NFL proportion adsorbed at the surface of LNC after incubation at room temperature during 30 sec or 1 h: A) Effect of Span80 content: 0, 27 and 54% (w/w_{Lab}) (NFL 0.05 mg/mL and neutral LNC); B) Effect of LNC surface charge: anionic, neutral and cationic (NFL 0.05 mg/mL and Span80 27% (w/w_{Lab})); and C) Effect of NFL concentration: 0.05, 0.1 and 0.15 mg/mL (with neutral and anionic LNC, Span80 27% (w/w_{Lab})) (n = 3, mean ± SD, * $p < 0.05$).

NFL in LNC-based hydrogels strengthens the mechanical properties of the hydrogels and improves the sustained release

Hydrogels were prepared by adding crosslinking agents (GemC12 or CytC16) to the anionic, neutral and cationic LNC described above. The peptide was added during the last cooling cycle, when the temperature reached 37°C. Cytotoxic GemC12 was used to study the anticancer properties of the hydrogels, while CytC16 allowed the investigation of cell interactions *in vitro*, and biodistribution studies *in vivo*.

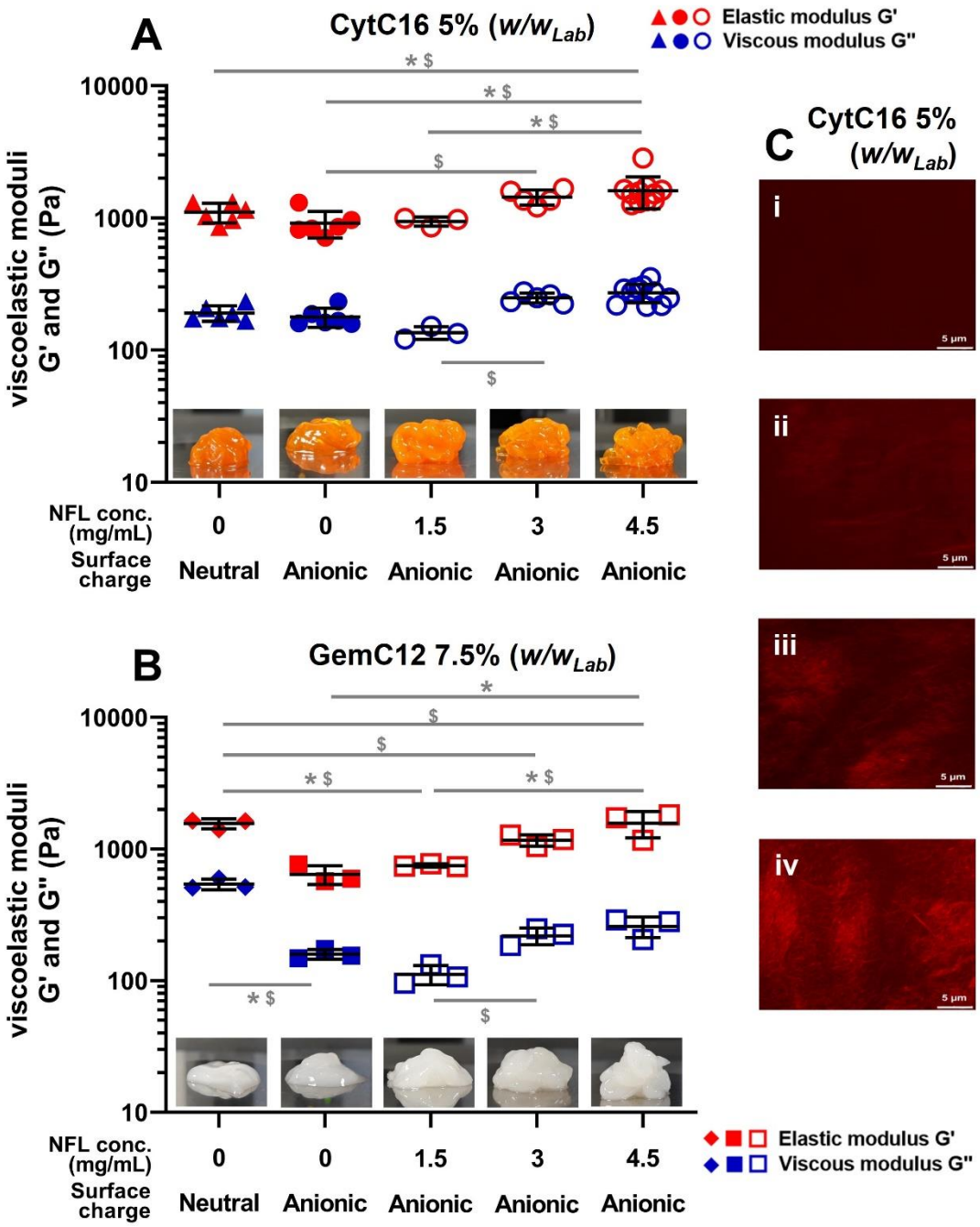

Figure 2. The mechanical properties of LNC-based hydrogels are enhanced by NFL. Viscoelastic properties: elastic (G') and viscous (G'') moduli and pictures of LNC-based hydrogels done with A) CytC16 5% or B) GemC12 7.5% (w/w_{Lab}) as crosslinking agents, *versus* NFL concentration (0 to 4.5 mg/mL) and LNC surface charge (anionic or neutral). DiA was loaded in LNC for the LNC-based hydrogels done with CytC16 in the picture. Oscillation frequency: 1 Hz, oscillatory strain amplitude: 0.1% (linear regimen), T = 25°C (n = 3–11, mean ± SD, G' comparison: * $p < 0.05$, G'' comparison: $ $p < 0.05$). C) **Visualization of LNC-based hydrogel network.** Confocal microscopy images for DiI-labelled anionic LNC-based hydrogels done with CytC16 5% (w/w_{Lab}) as crosslinking agent and various NFL concentrations: i) 0, ii) 1.5, iii) 3 and iv) 4.5 mg/mL.

All but one formulation afforded hydrogels, irrespective of the surface charge of the LNC (Anionic, neutral or cationic), the nature of the crosslinking agent (GemC12 or CytC16) or the concentration of NFL (0 to 4.5 mg/mL). The only formulation that formed a flowing viscous solution (not a gel) contained anionic LNC and was prepared with CytC16 2.5% (w/w_{Lab}), without NFL (Supplementary Figure S1). Generally, hydrogels containing anionic LNC had decreased mechanical properties compared to those formulated with neutral LNC: irrespective of the crosslinking agent, G' and G'' values decreased between 5 to 40% when hydrogels were prepared with anionic LNC, compared to their neutral counterpart (Figures 2A & 2B). However, the addition of NFL to these hydrogels restored their rigidity to values comparable to those obtained with neutral LNC. When the peptide concentration increased above 3 mg/mL, some mechanical properties were even enhanced in comparison to hydrogels with neutral LNC and no NFL, as measured by rheology or visual observation (Figure 2A and supplementary Figure S1). For example, anionic LNC-based hydrogels with CytC16 2.5% (w/w_{Lab}) and NFL at 4.5 mg/mL had G' and G'' values that were 1.7- and 1.9-fold higher than those prepared with neutral LNC without NFL. The effects of NFL on the rigidity of hydrogels were also confirmed with a higher concentration of CytC16 (5% (w/w_{Lab})) (Figure 2A). With NFL 4.5 mg/mL, hydrogels with CytC16 had a 1.4-fold increase in both G' and G'' compared to hydrogels prepared with neutral LNC (without peptide). The addition of 4.5 mg/mL of the peptide to hydrogels composed of neutral and cationic LNC also resulted in an increase in rigidity (Supplementary Figure S2). Altogether, these observations suggest that the NFL contributes to inter-particle interactions in the gel, which translates into a more rigid hydrogel. Observations under confocal microscopy confirmed that this increase in hydrogel rigidity was due to a network of LNC that becomes denser as the NFL concentration increases (Figure 2C).

The non-steady flow property of the LNC-based hydrogels were also studied with 2 cycles of increasing and decreasing controlled shear rates, ranging from 0.1 to 100 s^{-1}. For all types of hydrogels (anionic LNC, CytC16 or GemC12 as crosslinking agent, with or without NFL), shear thinning profiles were obtained. This decrease in viscosity upon the increase of the shear rate was non-thixotropic, as confirmed by the overlap of the curves observed upon increasing and decreasing the shear rate (Supplementary Figure S3). As for the already reported LNC-based hydrogel [25,26], the addition of NFL does not prevent the hydrogel from recovering all its strain after the application of a high stress such as administration through a syringe with a needle.

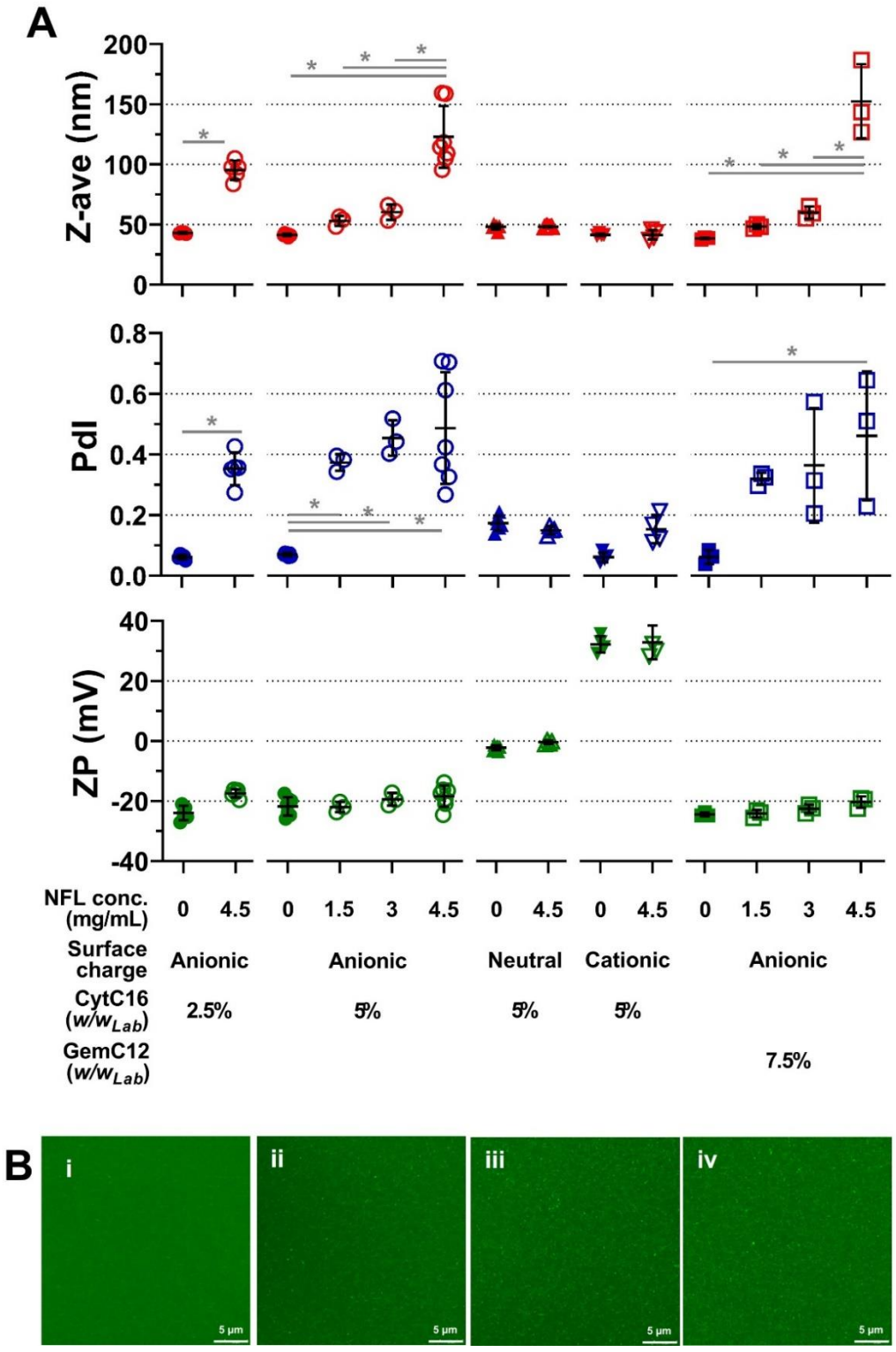

Figure 3. A) Size distribution of LNC before gelation is influenced by NFL. Size distribution (Z-average, Z-ave; and polydispersity index, PdI) and surface characteristics (Zeta potential, ZP) for LNC with various surface charges: anionic, neutral and cationic, loaded with CytC16 or GemC12 (2.5, 5% or 7.5% (w/w_{Lab})), with (1.5, 3 or 4.5 mg/mL) or without NFL, before the completion of gelation (n = 3–7, mean ± SD, * $p < 0.05$). **B) Size distribution of LNC after hydrogel dissolution is influenced by NFL.** Confocal microscopy images for DiA-labelled anionic LNC-based hydrogels done with CytC16 5% (w/w_{Lab}) and various NFL concentrations: i) 0, ii) 1.5, iii) 3 and iv) 4.5 mg/mL, after dissolution.

Next, we measured how the addition of NFL changed the size distributions of the LNC, before gelation. Before exposure to NFL, anionic and neutral LNC had initial diameters (Z-ave values) of about 40 nm and 50 nm, with monodispersed distributions (PdI < 0.1). With anionic LNC, the addition of NFL resulted in an increase in diameter with an increase in NFL concentration, irrespective of the crosslinking agent used or its concentration (Figure 3). In these conditions, the increase in PdI also indicated a loss of monodispersity and/or monomodality of the distribution, suggesting that association between LNC and the peptide could form clusters of LNC, before gelation. In comparison, neutral and cationic LNC maintained their original size distribution (*i.e.*, no change in Z-ave or PdI), even in the presence of NFL at 4.5 mg/mL. These results support that the slower and incomplete adsorption of the peptide on neutral and cationic LNC (observed in Figure 1B) prevents the formation of interparticle interactions before gelation. Again, confocal microscopy examination of the releasing media showed that increasing the NFL concentration in the hydrogel resulted in higher numbers of LNC clusters, after hydrogel dissolution (Figure 3B). Without NFL, LNC fluorescence remains diffuse (Figure 3Bi), but distinct fluorescent domains (*i.e.*, aggregates or clusters) appear as the peptide concentration increases (Figures 3Bii to 3Biv).

Next, we used fluorescence to evaluate the release profiles of DiA-labeled LNC from CytC16 crosslinked hydrogels. In the absence of NFL, the hydrogels containing anionic and cationic LNC had comparable release profiles, and dissolution occurred faster than with hydrogels containing neutral LNC (Figure 4A). These results confirmed our previous findings that release speed correlates with the mechanical properties of the hydrogels [26]. The addition of charge at the surface of LNC increases electrostatic repulsion, which competes with the crosslinking of the hydrogels; this results in a hydrogel with lower rigidity and faster release. The release profiles were not altered significantly upon the introduction of NFL to hydrogels containing neutral and positive LNC, reinforcing that the peptide shows limited interactions with these LNC. In contrast, when NFL was added to anionic LNC, the release was significantly slowed down, again supporting that the peptide contributes to the structure of the hydrogel in these conditions (Figure 4A). The effect of NFL on the release properties was also clearly perceived with gels containing GemC12 (Figure 4B). In these experiments using hydrogels with anionic LNC crosslinked with GemC12 7.5% (w/w_{Lab}), the release of the cytotoxic molecule, as quantified by HPLC, was more sustained in the presence of NFL.

To act as a targeting ligand, NFL must stay on the surface of the LNC after its release from the hydrogel. Hence, we documented the association between the peptide and LNC, once both have been released from the hydrogel (Figure 4C). With neutral and cationic LNC, only 20% of the released NFL remain associated with the nanoparticles after the hydrogel dissolution. These findings agree with those obtained with suspensions of LNC (Figure 1B) and suggest that gelation does not promote further interactions beyond those that are perceivable after 1 h of incubation. In contrast, the NFL remains strongly associated with anionic LNC after their release from the hydrogel (Figure 4C). In these conditions, with hydrogels crosslinked with CytC16, ~100% of the peptide remains on the LNC, while more than 80% remains on anionic LNC after release from a hydrogel crosslinked with GemC12. Again, using HPLC, the amounts of NFL and GemC12 released from the hydrogel were quantified simultaneously (Figure 4B). Some differences exist between the release rates of both molecules: for the first 24 h, NFL is released approximately 2.6-fold faster than GemC12. However, after this first initial burst release, the release rate of NFL decreases and becomes slower (approximately 1.6-fold

slower) than that of GemC12 (Figure 4D). These results suggest that in hydrogels containing NFL at 4.5 mg/mL, the distribution of the NFL might not be homogeneous, and that mainly clusters of NFL-rich LNC might be released earlier than LNC that contain a lower amount of peptide. Nevertheless, the strong association between the NFL and LNC at the end of the experiment support that active targeting might still occur after total hydrogel dissolution.

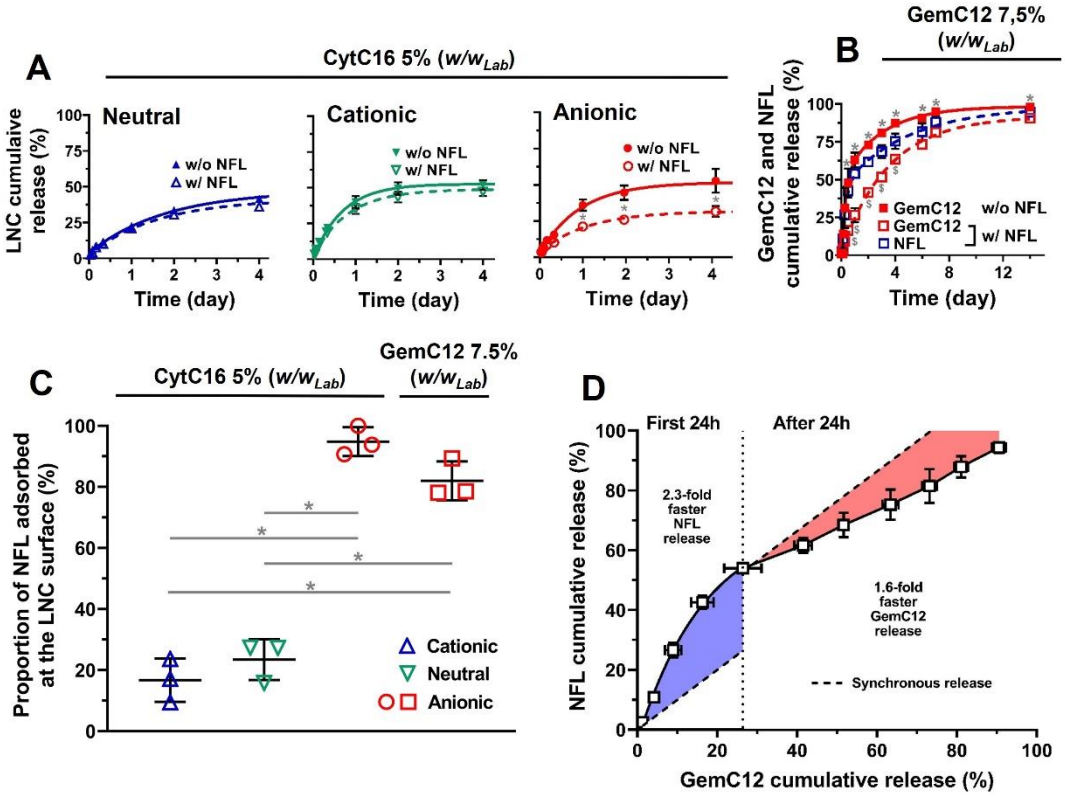

Figure 4. NFL enhanced the sustained release and remained totally associated to LNC after total hydrogel dissolution. A) Cumulative LNC release profiles from DiA-labelled neutral, cationic or anionic LNC-based hydrogels done with CytC16 5% (*w/w*$_{Lab}$) as crosslinking agent, with (4.5 mg/mL) or without NFL (n = 3, mean ± SD, * $p < 0.05$). B) Cumulative GemC12 and NFL release profiles from anionic LNC-based hydrogels done with GemC12 7.5% (*w/w*$_{Lab}$) as crosslinking agent, with (4.5 mg/mL) or without NFL (n = 3, mean ± SD, GemC12 comparison: * $p < 0.05$, GemC12 and NFL comparison: $ $p < 0.05$). C) Proportion of NFL adsorbed at the surface of LNC after the total dissolution of the DiA-labelled neutral, cationic or anionic LNC-based hydrogels, done with CytC16 5% or GemC12 7.5% (*w/w*$_{Lab}$) as crosslinking agents, with NFL peptide at 4.5 mg/mL (n = 3, mean ± SD; * $p < 0.05$). D) Correlation between the cumulative releases for both GemC12 and NFL, and comparison with synchronous cumulative releases, during the first 24 h and after 24 h (n = 3, mean ± SD). Release against PBS at 37°C with hydrogel/PBS ratio 1/7.5 (*v/v*).

NFL adsorbed at LNC surface after the release from the hydrogels allows the targeting of GBM cells and improved therapeutic efficacy *in vitro*

Using the DiA-labelled LNC, we examined the targeting capability of NFL-functionalized anionic LNC in GBM cancer cell lines (U-87 MG, F98, GL261) and healthy cells (NHA), after their release from the hydrogels. To do so, cell internalization was evaluated after the dissolution of hydrogels prepared with CytC16, and cytotoxicity was investigated with LNC released from GemC12-crosslinked formulations.

Results from flow cytometry and confocal microscopy experiments are presented in Figure 5 for hydrogels done with CytC16 5% (w/w_{Lab}) and supplementary Figure S4 for those done with CytC16 2.5% (w/w_{Lab}). These experiments show that for U-87 MG, F98 and GL261 cells, the NFL adsorbed at the surface of the LNC leads to faster cellular uptake in comparison with LNC without peptide. Specifically, after 3 h of incubation, NFL on the surface of LNC increased the proportion of fluorescent-positive cancer cells between 4.4- and 5-fold, compared to peptide-free nanoparticles; at that time, ~90% of U-87 MG and GL261 cells incubated with NFL-coated LNC were fluorescent. In comparison, F98 cells had lower internalization rates, with only 50% of the cells treated with NFL-adsorbed LNC being fluorescent. After 6 h of incubation, NFL still increased cellular internalization; however, the difference between formulations was reduced to 1.6- to 3-fold (Figure 5A). At that time, although almost 100% of cells incubated with NFL-coated LNC had become positive, internalization in the control group was also higher. For the F98 cell line, longer incubation resulted in cellular uptake by ~80% of the cells in contact with peptide-decorated LNC (*versus* 40% with control LNC). In contrast, the peptide did not increase internalization by healthy human astrocytes (NHA cell line), even after 6 h of incubation. At that time, less than 2% of NHA cells were fluorescent, regardless of peptide functionalization or incubation times (Figure 5A). These results were almost superimposable with those obtained gels containing a lower amount of crosslinking agents (*i.e.*, CytC16 2.5% (w/w_{Lab})) (Supplementary Figure S4). Finally, confocal microscopy experiments confirmed these results with the prominent visualization of LNC-related fluorescence in GBM cells when NFL peptide is present, and a complete absence of LNC-related fluorescence for NHA cells, with or without NFL (Figure 5B). Altogether these results strongly support that 1) NFL continues to act as a targeting peptide even after the release of LNC from the hydrogel, and 2) NFL-targeting appears to be specific toward GBM cancer cells. The mechanism by which NFL increases internalization has yet to be fully elucidated, but the process appears to involve tyrosine kinase receptors [39], which are overexpressed in GBM cells [43-46]. Other explanations could involve differences in proliferation [39] or plasma membrane composition and fluidity between GBM and healthy cell lines [47-49].

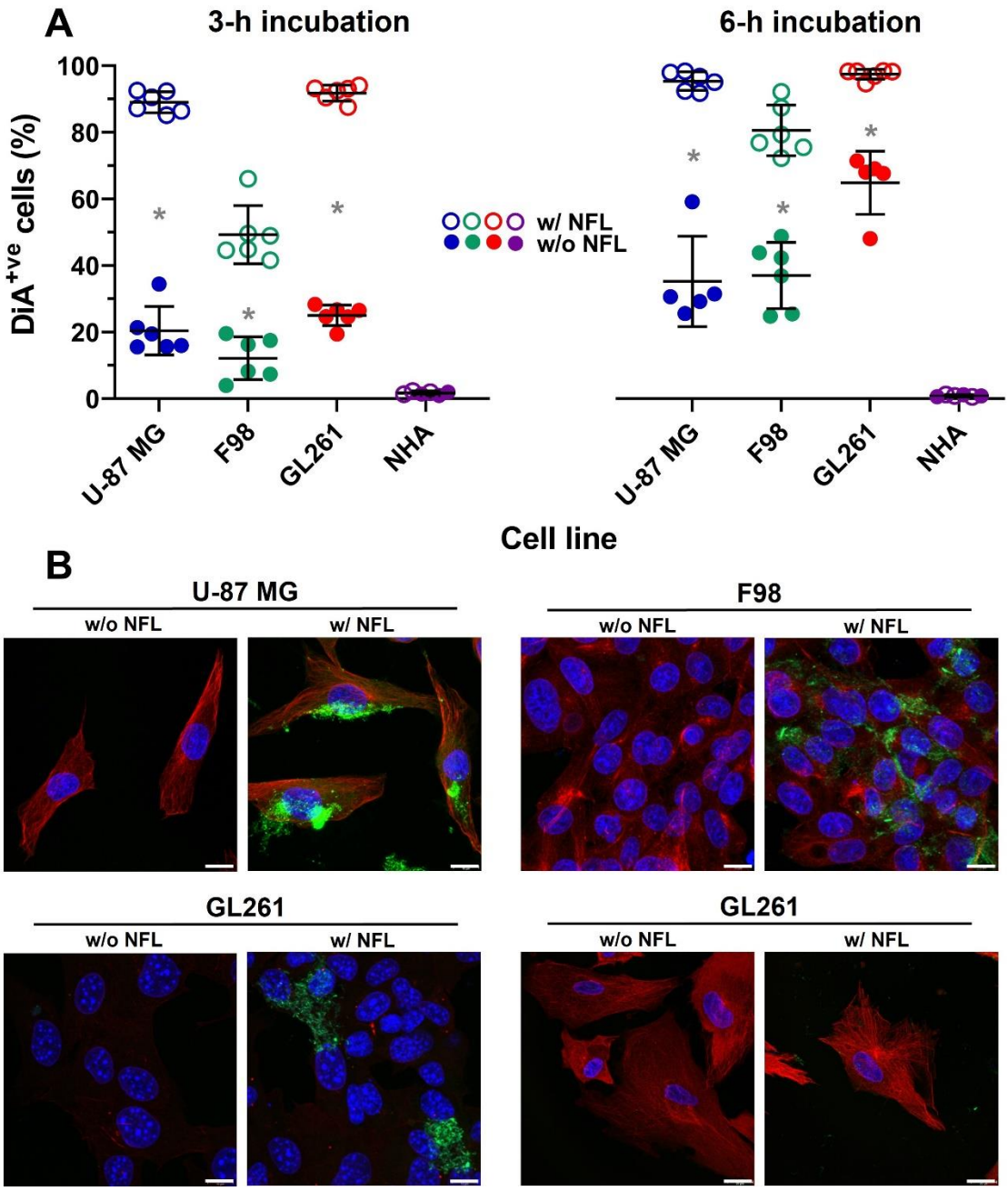

Figure 5. The LNC associated with NFL, released from the hydrogel, are faster internalized. A) DiA-positive cells for U-87 MG, F98, GL261 and NHA cell lines after 3-h or 6-h incubation with LNC without or associated with NFL (4.5 mg/mL), obtained after the total dissolution of the DiA-labelled anionic LNC-based hydrogel done with CytC16 5% (w/w_{Lab}) (n = 3-6; mean ± SD; * $p < 0.05$). B) Confocal microscopy images for U-87 MG, F98, GL261 (scale bars = 10 µm) and NHA cell line (scale bar = 20 µm), after 3-h incubation with LNC without or associated with NFL (4.5 mg/mL), obtained after the total dissolution of the DiI-labelled anionic LNC-based hydrogel done with CytC16 5% (w/w_{Lab}). Blue corresponds to DAPI staining of the nucleus, red to α-tubulin staining with an Alexa Fluor™ 647-coupled antibody, and green to DiI-labelled LNC (Separated channels can be visualized in supplementary Figure S5).

Next, we evaluated whether this increase in cellular uptake translated into increased antiproliferative activity, using the cytotoxic GemC12 crosslinking agent. This time, the LNC with or without NFL 4.5 mg/mL, incubated with cells, were obtained by the dissolution of hydrogels prepared with GemC12 7.5% (w/w_{Lab}). In light of internalization studies, cells were incubated with LNC for short time (lower than 6 h), and then washed, before evaluating cell survival, 24 to 48 h after. In this context, the ability of the NFL to enhance the cytotoxicity of GemC12 seems to be cell dependent (Figure 6). In U-87 MG cells, decoration of LNC with NFL significantly decreased the median effective concentration (EC_{50}) compared to peptide-free LNC. Specifically in these cells, the EC_{50} value of GemC12 significantly decreased from 0.19 ± 0.01 to 0.14 ± 0.01 µg/mL, when LNC were coated with NFL. In the same conditions in F98 cells, we also observed a non-significant decrease in EC_{50}, from 0.46 ± 0.17 to 0.37 ± 0.11 µg/mL. While the increased internalization in these two cell lines can explain this enhancement in cytotoxicity, the presence of NFL at the surface of LNC did not improve efficacy in GL261 cells. In this context, the EC_{50} values of GemC12 were similar irrespective of the presence of NFL: 0.11 ± 0.06 and 0.11 ± 0.01 µg/mL. Finally, controls in healthy astrocytes (NHA cells) cultured in the same conditions highlighted EC_{50} values for GemC12 that were higher than 10 µg/mL, irrespective of the presence of NFL. These results are in accordance with cellular uptake studies showing no LNC internalization by NHA cells, after 6 h of incubation.

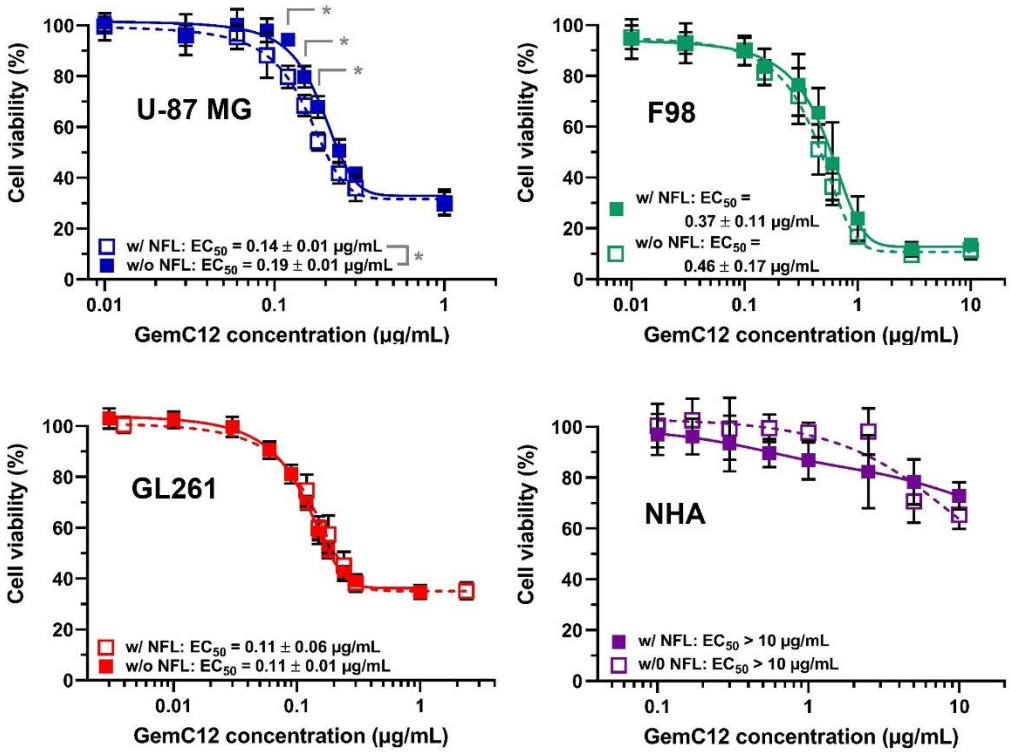

Figure 6. The cytotoxicity of GemC12 is enhanced when LNC is associated with NFL after LNC-based hydrogel dissolution in U-87 MG cells. Cell viability (resazurin assay) *versus* the GemC12 concentration for U-87 MG, F98, GL261 and NHA cell lines. The cells were treated with LNC without or associated with NFL (4.5 mg/mL), obtained after the total dissolution of the anionic LNC-based hydrogel done with GemC12 7.5% (w/w_{Lab}) (n = 3-6; mean ± SD; * $p < 0.05$).

It remains unclear why the benefits of NFL targeting vary between cell type. GemC12 is a prodrug that requires multiple enzymatic transformations to reach its active form, gemcitabine triphosphate. This cascade involves deoxycytidine kinase (dCK), nucleoside monophosphate kinase and diphosphate kinase [50]. Expression and activity of dCK are biomarkers of gemcitabine efficacy in GBM [51], and differences in sensitivity to gemcitabine was already reported between GBM cell lines [29]. GL261 seem to be slightly more sensitive to GemC12 than U-87 MG (*i.e.*, EC_{50} 1.7-fold lower). This could explain why addition of NFL does not significantly increase LNC toxicity

NFL-targeting increases LNC distribution to cancer cells *in vivo,* and NFL-containing hydrogels delay GBM recurrences in an orthotopic tumor resection model.

To evaluate if the NFL could increase LNC targeting to residual cancer cells *in vivo*, we used a mouse model of tumor resection from GBM orthotopic xenografts (U-87 MG cell line) established by our team [29,41]. In alignment with clinical practice, 14 days after implantation of GBM cells, mice underwent surgery to partially remove the tumor, and the resection cavity was filled with LNC-based hydrogels.

To investigate *in vivo* efficacy, the resection cavity was filled with cytotoxic anionic LNC-based hydrogels prepared with GemC12 7.5% (w/w_{Lab}), with or without NFL 4.5 mg/mL. After surgery, mice were monitored daily (not blinded observations) and sacrificed when the ethical points were reached (Figure 7A). The median survival of the control group (non-treated mice) was found to be 38 days, with the last mouse sacrificed at 73 days. This control group confirmed the repeatability of the model that we have been implementing for several years [29,41]. Using the LNC-based hydrogel without NFL, the median survival was increased to 44 days, with 1 in 8 mice considered long-lived (> 110 days). Using the LNC-based hydrogel with NFL, the median survival was significantly increased to 74 days ($p = 0.0108$ compared to the control group, and $p = 0.0460$ compared to the LNC-based hydrogel without NFL group), with 2 in 8 mice considered long-lived (> 110 days) (Figure 7B). While the difference in *in vitro* cytotoxic activity was not so striking (but significant), certainly due to the short incubation time to enhance the targeting of GBM cells by NFL, the progressive release of the LNC from the hydrogels strengthened the active targeting, and so allowed longer survival time with NFL. Previously, using the same repeatable mouse model of tumor resection from GBM orthotopic xenografts, we already reported the *in vivo* anti-tumor efficacy of neutral LNC-based hydrogel done with GemC12 at the same dose and without NFL, resulting in a median survival of 62 days [29]. The *in vivo* data we obtained with the two current implants we developed can be explained in relation to the previous one. Using anionic LNC-based hydrogel, the release of the non-targeting anionic LNC is faster than that of the non-targeting neutral LNC (figure 4A), leading to a less sustained release and so a decrease in the median survival (44 *versus* 62 days, respectively). If we compare now with the targeting anionic LNC, the slower release (figure 4A) combined to the GBM targeting efficacy with NFL (Figure 5A) led to a longer median survival (73 *versus* 62 days, respectively).

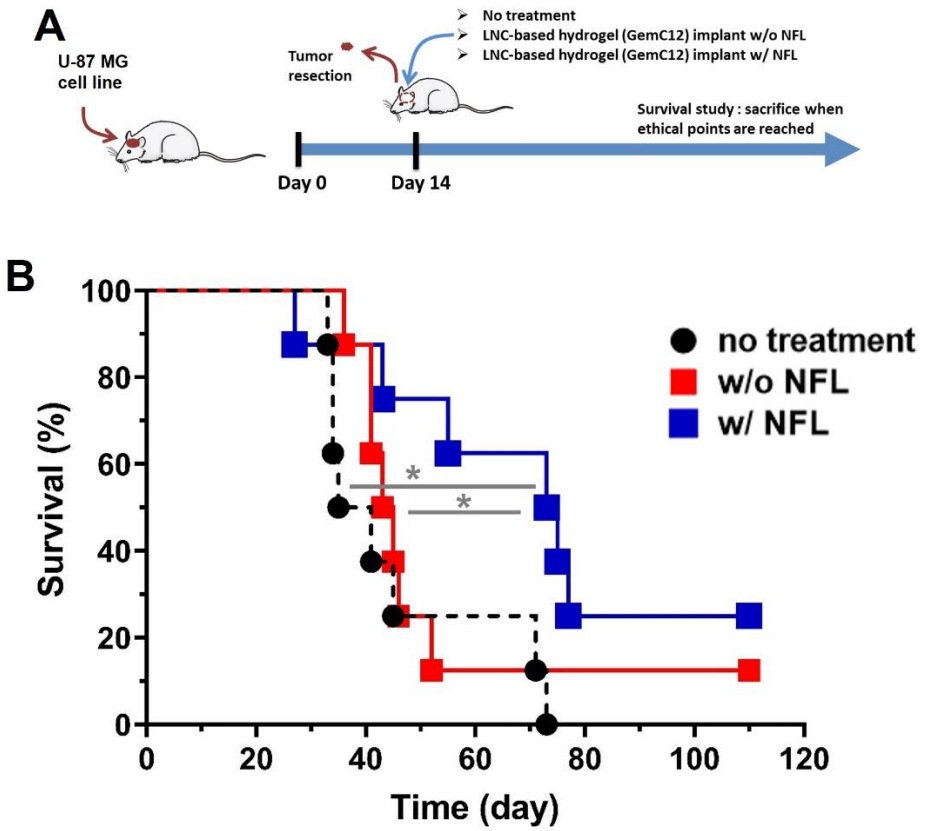

Figure 7. The survival of mice is enhanced when NFL is associated to LNC-based hydrogel, after its implantation in the resection cavity of the orthotopic GBM model. A) Time schedule of the anti-tumor efficacy using a U-87 MG orthotopic tumor mouse model. B) Kaplan–Meier survival curves for mice non-treated or treated with anionic LNC-based hydrogels hydrogel done with GemC12 7.5% (w/w_{Lab}) with or without NFL 4.5 mg/mL, implanted in the resection cavity (n = 8; * $p < 0.05$).

To confirm the role of NFL on the biodistribution of LNC, the resection cavity was filled with fluorescent anionic LNC hydrogels prepared with CytC16 5% (w/w_{Lab}), with or without NFL 4.5 mg/mL. Six days after surgery and implantation, tissues were collected and analyzed with confocal microscopy to visualize the presence of DiD-labelled LNC (Figure 8A). This time corresponds to the difference between the median survivals for the untreated group of mice and the group of mice that received the hydrogel implant without NFL (i.e., 38 *versus* 44 days) (Figure 7). Six days after implantation, DiD-labelled LNC were still detectable in the brain tissue, irrespective of the presence of NFL (Figure 8B). However, LNC with NFL localized with brighter intensity, close to the resection cavity, near remaining tumor cells. In contrast, LNC without NFL were detected further far from the resection cavity, suggesting increased diffusion within the brain. The relative distance and intensity of DiD-positive pixels in the images were calculated by image analysis. LNC without NFL were on average 5-fold more distant from the resection cavity than their targeted counterpart (Figure 8C). This difference in the LNC localization does not impact the profiles for the fluorescence intensity of individual DiD-positive pixels relatively similar for the four mice (Figure 8D). Altogether, these results suggest that the peptide contributes to the local targeting of residual cancer cells, which could explain its increased efficacy.

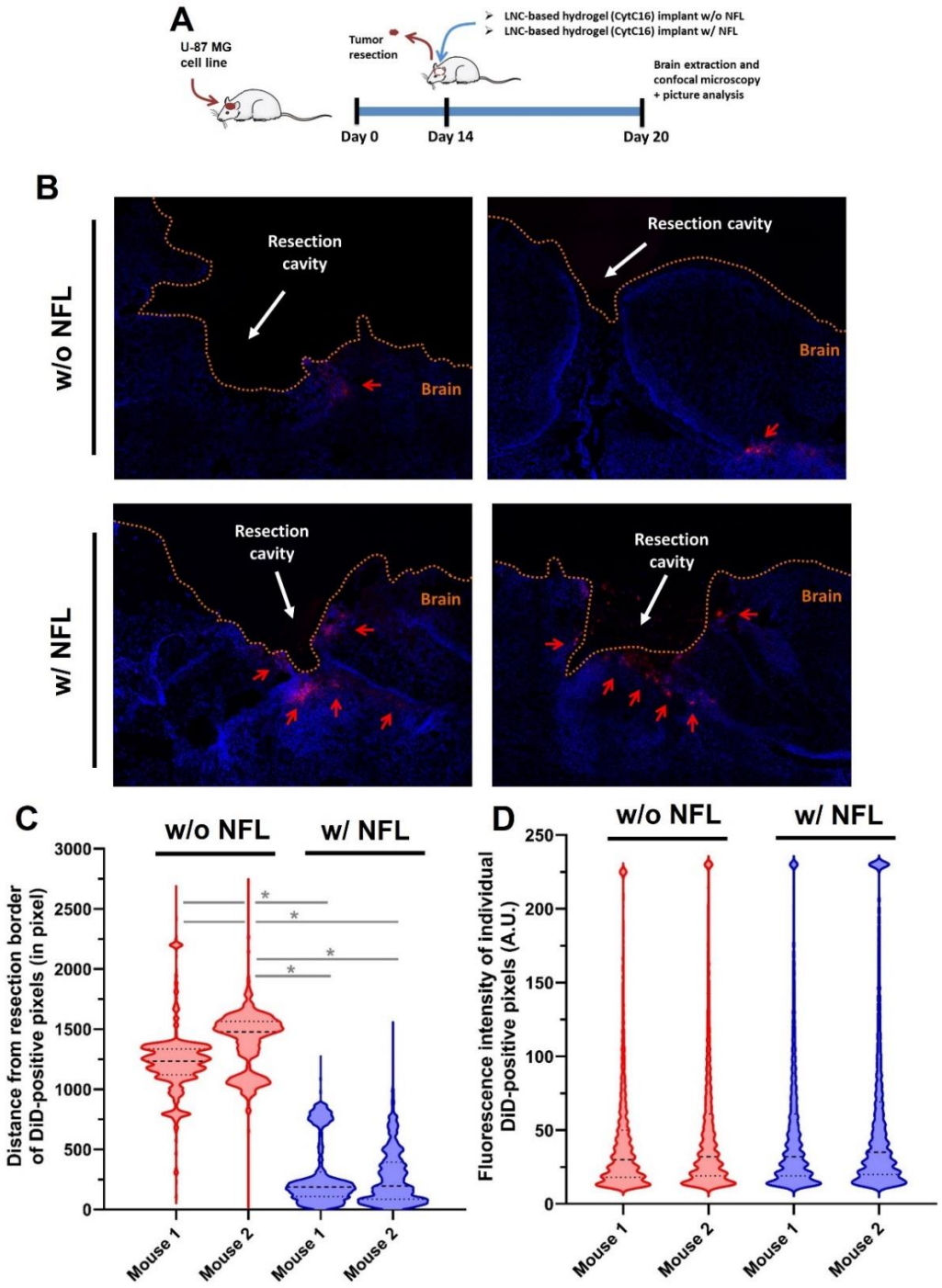

Figure 8. The LNC are better distributed at the periphery of the resection cavity when NFL is associated to LNC-based hydrogel, after its implantation in the resection cavity of the orthotopic GBM model. A) Time schedule of the LNC brain distribution using a U-87 MG orthotopic tumor mouse model. B) Confocal microscopy images (blue corresponds to DAPI staining of the nucleus and red to DiD (with red arrows)) of brain slices, 6 days after the implantation in the resection cavity of DiD-labelled anionic LNC-based hydrogels done with CytC16 5% (w/w_{Lab}) with or without NFL 4.5 mg/mL. C) Distance from the resection border of DiD-positive pixels and D) fluorescence intensities of individual DiD-positive pixels, obtained after the analyses of confocal microscopy image of brain slices, 6 days after the implantation in the resection cavity of DiD-labelled anionic LNC-based hydrogels done with CytC16 5% (w/w_{Lab}) with or without NFL 4.5 mg/mL (median ± quartiles; * $p < 0.05$).

Overall comments.

Despite improvements in the clinical management of GBM, these aggressive brain tumors remain deadly, and novel treatments are necessary. Given the current standard of care involving surgery, implantable technologies are particularly attractive. The present project builds on the successes of local administration to deliver a gemcitabine derivative, while circumventing the lack of specificity and lack of adaptation to the resection cavity geometry of Gliadel® wafers.

To increase treatment specificity, the NFL was chosen for its ability to target GBM cells [37-39] and the ease of functionalizing the peptide at the surface of LNC in suspension [34,35]. However, the incorporation of the peptide into the hydrogel required a systematic redesign of the formulation. In the present work, we maximized LNC-peptide interactions by using negatively charged LNC. While these changes resulted in variations in the viscoelastic properties of the hydrogels, interactions between the nanoparticles and the peptide afforded rigid gels with sustained delivery properties. Importantly, changes in composition also allowed LNC released from the hydrogel to maintain their interactions with the targeting peptide, which increased their ability to be rapidly internalized by GBM cells. *In vivo*, this higher tropism for cancer cells could result in localization of NFL-functionalized LNC near the resection cavity, 6 days after tumor resection and gel implantation. Treatment with NFL-decorated LNC also resulted in increased the median survival in animals, compared to LNC without the peptide. Altogether, this demonstration confirms the potential of combining local delivery and active targeting to treat GBM.

While the hydrogels presented herein are not curative on their own, they pave the way for new perspectives to improve the management of patients with GBM. GBM is an aggressive, highly infiltrative and heterogeneous cancer. Current treatment involves radiotherapy and the use of the alkylating agent, temozolomide, both exerting antiproliferative effects through DNA damage. Strong synergy might be obtained by combining these treatments with targeted gemcitabine-loaded LNC that stop DNA replication. The hydrogels might also provide an interesting alternative to differentially impact the different cells found in the GBM tumor microenvironment: cancer and stem cells, the endothelium, fibroblasts and inflammatory cells [52,53], as well as to use various drugs with complementary pharmacological activities [31,54]. The ability to sustain drug exposure to these important components of brain tumors might provide interesting ways of regulating cell growth and tumorigenic processes (angiogenesis, lymphangiogenesis and inflammation). Further work will establish how to better exploit the properties of these gels, notably by exploring different chemotherapeutic agents, targeting ligands and possible synergies with the Stupp protocol.

Conclusion

To summarize, a hydrogel of self-associated gemcitabine-loaded LNC able to target GBM cells was developed. The adsorption of the NFL: the GBM targeting peptide, at the surface of the LNC was possible with a relevant LNC surface modification. This association does not prevent the LNC from combining to form the hydrogel. In fact, it enhances the mechanical properties of the hydrogel, enabling even more the sustained release of LNC than with hydrogels without NFL. Because the

association is maintained during the LNC release, we proved that the active and specific targeting of GBM cells by NFL-functionalized LNC is possible, thereby enhancing the antitumor effect *in vitro*. The enhanced antitumor effect was also confirmed *in vivo* using the hydrogel as an implant in a GBM resection mouse model. The median survival was significantly delayed in comparison to the hydrogel without targeting capacity, explained by a better localization of the therapeutics at the border of the resection cavity. In this way, we have demonstrated that the concept of targeted, local and sustained drug delivery system is relevant for the treatment of GBM. It offers promising perspectives for combination with the Stupp's protocol to ensure continuity in treatment between surgery and radiochemotherapy for patients with GBM. For future aspects, several considerations will be addressed relating to drug combinations with TMZ to highlight synergies for a better GBM patient standard of care.

Declaration of competing interest

The author Guillaume Bastiat is one of the inventors who patented the LNC-based hydrogel technology used in the article (WO2019048649A1). In addition, the authors Claire Gazaille and Adélie Mellinger are currently working in the GlioCure company which holds the patent license on the targeting peptide used in this article (WO2011073207A1).

Acknowledgments

This work was carried out within the research program of GLIOGEL (EuroNanoMed3 - 7th call), a multinational program supported by *Agence Nationale de la Recherche* (France), *Fonds National de la Recherche Scientifique* (Belgium), and the *Fonds de Recherche du Québec – Santé* (Quebec, Canada). The authors also thank the « *Fondation ARC pour la Recherche sur le Cancer* » and the « *Ligue Contre le Cancer* (Comité du Maine-et-Loire) » and *Fonds de la Recherche Scientifique—Fonds National de la Recherche Scientifique* (grant agreement nos. 33669945, 40003419 for their financial supports). Neda Madadian-Bozorg acknowledges a scholarship from the *Fonds d'Enseignement et de Recherche* of the Faculty of Pharmacy of Université Laval. Nicolas Bertrand is a Junior 2 Fellow of the *Fonds de Recherche du Québec – Santé*. We are also grateful to the SCAHU, PACEM and SCIAM platforms (SFR ICAT 4208 from Angers University) for the use of their animal facilities and for their technical supports.

References

[1] D.N. Louis, A. Perry, P. Wesseling, D.J. Brat, I.A. Cree, D. Figarella-Branger, The 2021 WHO classification of tumors of the central nervous system: a summary, Neuro Oncol. 23 (2021) 1231-1251, https://doi.org/10.1093/neuonc/noab106.

[2] Q.T. Ostrom, N. Patil, G. Cioffi, K. Waite, C. Kruchko, J.S. Barnholtz-Sloan, CBTRUS statistical report: primary brain and other central nervous system tumors diagnosed in the United States in 2013-2017, Neuro Oncol. 22 (2021) iv1-96, https://doi.org/10.1093/neuonc/noab200.

[3] K.D. Miller, Q.T. Ostrom, C. Kruchko, N. Patil, T. Tihan, G. Cioffi, Brain and other central nervous system tumor statistics, 2021, CA Cancer J. Clin. 71 (2021) 381-406, https://doi.org/10.3322/caac.21693.

[4] B.M. Alexander, T.F. Cloughesy, Adult Glioblastoma, J. Clin. Oncol. 35 (2017) 2402–2409, https://doi.org/10.1200/JCO.2017.73.0119.

[5] R. Stupp, W.P. Mason, M.J. van den Bent, M. Weller, B. Fisher, M.J. Taphoorn, Radiotherapy plus concomitant and adjuvant temozolomide for glioblastoma, N. Engl. J. Med. 352 (2005) 987-996, https://doi.org/10.1056/NEJMoa043330.

[6] E. Feng, C. Sui, T. Wang, G. Sun G, Temozolomide with or without radiotherapy in patients with newly diagnosed glioblastoma multiforme: a meta-analysis, Eur. Neurol. 77 (2017) 201-210, https://doi.org/10.1159/000455842.

[7] M. Rapp, J. Baernreuther, B. Turowski, H.J. Steiger, M. Sabel, M.A. Kamp, Recurrence pattern analysis of primary glioblastoma, W. Neurosurg. 103 (2017) 733-740, https://doi.org/10.1016/j.wneu.2017.04.053.

[8] S. Reddy, K. Tatiparti, S. Sau, A.K, Recent advances in nano delivery systems for blood-brain barrier (BBB) penetration and targeting of brain tumors, Drug Discov. Today 26(8) (2021) 1944-1952, https://doi.org/10.1016/j.drudis.2021.04.008.

[9] A. Picca, D. Guyon, O.S. Santonocito, C. Baldini, A. Idbaih, A. Carpentier, A.G. Naccarato, M. Caccese, G. Lombardi, A.L. Di Stefano, Innovating Strategies and Tailored Approaches in Neuro-Oncology, Cancers (Basel) 14(5) (2022) 1124, https://doi.org/10.3390/cancers14051124.

[10] J.W. Roberts, L. Powlovich, N. Sheybani, S. LeBlang, Focused ultrasound for the treatment of glioblastoma, J. Neurooncol. 157(2) (2022) 237-247, https://doi.org/10.1007/s11060-022-03974-0.

[11] M. Alghamdi, M. Gumbleton, B. Newland, Local delivery to malignant brain tumors: potential biomaterial-based therapeutic/adjuvant strategies, Biomater. Sci. 9(18) (2021) 6037-6051, https://doi.org/10.1039/d1bm00896j.

[12] T.S. van Solinge, L. Nieland, E.A. Chiocca, M.L.D. Broekman, Advances in local therapy for glioblastoma - taking the fight to the tumour, Nat. Rev. Neurol. 18(4) (2022) 221-236, https://doi.org/10.1038/s41582-022-00621-0.

[13] C. Bastiancich, A. Malfanti, V. Préat, R. Rahman, Rationally designed drug delivery systems for the local treatment of resected glioblastoma, Adv. Drug Deliv. Rev. 177 (2021) 113951, doi: 10.1016/j.addr.2021.113951.

[14] C. Bastiancich, E. Bozzato, I. Henley, B. Newland, Does local drug delivery still hold therapeutic promise for brain cancer? A systematic review, J. Control. Release 337 (2021) 296-305, https://doi.org/10.1016/j.jconrel.2021.07.031.

[15] H. Brem, M.S. Mahaley, N.A. Vick, K.L. Black, S.C. Schold, P.C. Burger, Interstitial chemotherapy with drug polymer implants for the treatment of recurrent gliomas, J. Neurosurg. 74 (1991) 441-446, https://doi.org/10.3171/jns.1991.74.3.0441.

[16] E. Mathiowitz, W.M. Saltzman, A. Domb, P. Dor, R. Langer, Polyanhydride microspheres as drug carriers. II. microencapsulation by solvent removal, J. Appl. Polym. Sci. 35 (1988) 755-774, https://doi.org/10.1002/app.1988.070350316.

[17] M.J. McGirt, K.D. Than, J.D. Weingart, K.L. Chaichana, F.J. Attenello, A. Olivi, J. Laterra, L.R. Kleinberg, S.A. Grossman, H. Brem, A. Quiñones-Hinojosa, Gliadel (BCNU) wafer plus concomitant temozolomide therapy after primary resection of glioblastoma multiforme, J. Neurosurg. 110 (2009) 583-588, https://doi.org/10.3171/2008.5.17557.

[18] L.S. Ashby, K.A. Smith, B. Stea, Gliadel wafer implantation combined with standard radiotherapy and concurrent followed by adjuvant temozolomide for treatment of newly diagnosed high-grade glioma: a systematic literature review, World J. Surg. Oncol. 14 (2016) 225, https://doi.org/10.1186/s12957-016-0975-5.

[19] J. Perry, A. Chambers, K. Spithoff, N. Laperriere, Gliadel wafers in the treatment of malignant glioma: a systematic review, Curr. Oncol. 14 (2007) 189-194, https://doi.org/10.3747/co.2007.147.

[20] W. Xing, C. Shao, Z. Qi, C. Yang, Z. Wang, The role of gliadel wafers in the treatment of newly diagnosed GBM: a meta-analysis, Drug Des. Devel. Ther. 9 (2015) 3341-3348, https://doi.org/10.2147/DDDT.S85943.

[21] D.A. Bota, A. Desjardins, J.A. Quinn, M.L. Affronti, H.S. Friedman, Interstitial chemotherapy with biodegradable BCNU (Gliadel) wafers in the treatment of malignant gliomas, Ther. Clin. Risk Manag. 3 (2007) 707-715.

[22] A.J. Domb, Polymeric carriers for regional drug therapy, Mol. Med. Today 1 (1995) 134-139, https://doi.org/10.1016/S1357-4310(95)80091-3.

[23] S.A. Grossman, C. Reinhard, O.M. Colvin, M. Chasin, R. Brundrett, R.J. Tamargo, The intracerebral distribution of BCNU delivered by surgically implanted biodegradable polymers, J. Neurosurg. 76 (1992) 640-647, https://doi.org/10.3171/jns.1992.76.4.0640.

[24] L.K. Fung, M.G. Ewend, A. Sills, E.P. Sipos, R. Thompson, M. Watts, Pharmacokinetics of interstitial delivery of carmustine, 4-hydroperoxycyclophosphamide, and paclitaxel from a biodegradable polymer implant in the monkey brain, Cancer Res. 58 (1998) 672-684.

[25] E. Moysan, Y. González-Fernández, N. Lautram, J. Béjaud, G. Bastiat, J.P. Benoit, An innovative hydrogel of gemcitabine-loaded lipid nanocapsules: when the drug is a key player of the nanomedicine structure, Soft Matter 10 (2014) 1767-1777. https://doi.org/10.1016/10.1039/c3sm52781f.

[26] M. Pitorre, C. Gazaille, L.T.T. Pham, K. Frankova, J. Béjaud, N. Lautram, J. Riou, R. Perrot, F. Geneviève, V. Moal, J.P. Benoit, G. Bastiat, Polymer-free hydrogel made of lipid nanocapsules, as a local drug delivery platform, Mater. Sci. Eng. C Mater. Biol. Appl. 126 (2021) 112188, https://doi.org/10.1016/j.msec.2021.112188.

[27] M. Pitorre, H. Gondé, C. Haury, M. Messous, J. Poilane, D. Boudaud, E. Kanber, G.A. Rossemond Ndombina, J.P. Benoit, G. Bastiat, Recent advances in nanocarrier-loaded gels: which drug delivery technologies against which diseases?, J. Control. Release 266 (2017) 140-155, https://doi.org/10.1016/j.jconrel.2017.09.031.

[28] N. Wauthoz, G. Bastiat, E. Moysan, A. Cieślak, K. Kondo, M. Zandecki, V. Moal, M.C. Rousselet, J. Hureaux, J.P. Benoit, Safe lipid nanocapsule-based gel technology to target lymph nodes and combat mediastinal metastases from an orthotopic non-small-cell lung cancer model in SCID-CB17 mice, Nanomedicine 11(5) (2015) 1237-1245, https://doi.org/10.1016/j.nano.2015.02.010.

[29] C. Bastiancich, J. Bianco, K. Vanvarenberg, B. Ucakar, N. Joudiou, B. Gallez, G. Bastiat, F. Lagarce, V. Préat, F. Danhier, Injectable nanomedicine hydrogel for local chemotherapy of glioblastoma after surgical resection, J. Control. Release 264 (2017) 45-54, https://doi.org/10.1016/j.jconrel.2017.08.019

[30] C. Bastiancich, L. Lemaire, J. Bianco, F. Franconi, F. Danhier, V. Préat, G. Bastiat, F. Lagarce, Evaluation of lauroyl-gemcitabine-loaded hydrogel efficacy in glioblastoma rat models, Nanomedicine (Lond) 13 (2018) 1999-2013, https://doi.org/10.2217/nnm-2018-0057.

[31] C. Bastiancich, E. Bozzato, U. Luyten, F. Danhier, G. Bastiat, V. Préat, Drug combination using an injectable nanomedicine hydrogel for glioblastoma treatment, Int. J. Pharm. 559 (2019) 220-227, https://doi.org/10.1016/j.ijpharm.2019.01.042.

[32] C. Bastiancich, K. Vanvarenberg, B. Ucakar, M. Pitorre, G. Bastiat, F. Lagarce, V. Préat, F. Danhier, Lauroyl-gemcitabine-loaded lipid nanocapsule hydrogel for the treatment of glioblastoma, J. Control. Release 225 (2016) 283-293, https://doi.org/10.1016/j.jconrel.2016.01.054.

[33] C. Gazaille, M. Sicot, P. Saulnier, J. Eyer, G. Bastiat, Local Delivery and Glioblastoma: Why Not Combining Sustained Release and Targeting?, Front. Med. Technol. 3 (2021) 791596, https://doi.org/10.3389/fmedt.2021.791596.

[34] J. Balzeau, M. Pinier, R. Berges, P. Saulnier, J.P. Benoit, J. Eyer, The effect of functionalizing lipid nanocapsules with NFL-TBS.40-63 peptide on their uptake by glioblastoma cells, Biomaterials 34(13) (2013) 3381-3389, https://doi.org/10.1016/j.biomaterials.2013.01.068.

[35] D. Carradori, P. Saulnier, V. Préat, A. des Rieux, J. Eyer, NFL-lipid nanocapsules for brain neural stem cell targeting in vitro and in vivo, J. Control. Release 238 (2016) 253-262, https://doi.org/10.1016/j.jconrel.2016.08.006.

[36] A. Bocquet, R. Berges, R. Frank, P. Robert, A.C. Peterson, J. Eyer, Neurofilaments bind tubulin and modulate its polymerization, J. Neurosci. 29(35) (2009) 11043-11054, https://doi.org/10.1523/JNEUROSCI.1924-09.2009.

[37] R. Berges, J. Balzeau, M. Takahashi, C. Prevost, J. Eyer, Structure-function analysis of the glioma targeting NFL-TBS.40-63 peptide corresponding to the tubulin-binding site on the light neurofilament subunit, PLoS One 7(11) (2012) e49436, https://doi.org/10.1371/journal.pone.0049436.

[38] R. Berges, J. Balzeau, A.C. Peterson, J. Eyer, A tubulin binding peptide targets glioma cells disrupting their microtubules, blocking migration, and inducing apoptosis, Mol. Ther. 20(7) (2012) 1367-1377, https://doi.org/10.1038/mt.2012.45.

[39] C. Lépinoux-Chambaud, J. Eyer, The NFL-TBS.40-63 anti-glioblastoma peptide enters selectively in glioma cells by endocytosis, Int. J. Pharm. 454(2) (2013) 738-747, https://doi.org/10.1016/j.ijpharm.2013.04.004.

[40] C. Gazaille, M. Sicot, M. Akiki, N. Lautram, A. Dupont, P. Saulnier, J. Eyer, G. Bastiat, Characterization of Biological Material Adsorption to the Surface of Nanoparticles without a Prior Separation Step: a Case Study of Glioblastoma-Targeting Peptide and Lipid Nanocapsules, Pharm. Res. 38(4) (2021) 681-691, https://doi.org/10.1007/s11095-021-03034-8.

[41] M. Zhao, E. Bozzato, N. Joudiou, S. Ghiassinejad, F. Danhier, B. Gallez, V. Préat, Codelivery of paclitaxel and temozolomide through a photopolymerizable hydrogel prevents glioblastoma recurrence after surgical resection, J. Control. Release 309 (2019) 72-81, https://doi.org/10.1016/j.jconrel.2019.07.015.

[42] J. Bianco, C. Bastiancich, N. Joudiou, B. Gallez, A. des Rieux, F. Danhier, Novel model of orthotopic U-87 MG glioblastoma resection in athymic nude mice, J. Neurosci. Methods 284 (2017) 96-102, https://doi.org/10.1016/j.jneumeth.2017.04.019

[43] Y. Hamaoka, M. Negishi, H. Katoh, EphA2 Is a Key Effector of the MEK/ERK/RSK Pathway Regulating Glioblastoma Cell Proliferation, Cell. Signal. 28(8) (2016) 937-945, https://doi.org/10.1016/j.cellsig.2016.04.009.

[44] S.A. Shein, I.I. Kuznetsov, T.O. Abakumova, P.S. Chelushkin, P.A. Melnikov, A.A. Korchagina, D.A. Bychkov, I.F. Seregina, M.A. Bolshov, A.V. Kabanov, V.P. Chekhonin, N.V. Nukolova, VEGF- and VEGFR2-Targeted Liposomes for Cisplatin Delivery to Glioma Cells, Mol. Pharm. 13(11) (2016) 3712-3723, https://doi.org/10.1021/acs.molpharmaceut.6b00519.

[45] P.C. de Souza, N. Smith, R. Pody, T. He, C. Njoku, R. Silasi-Mansat, F. Lupu, B. Meek, H. Chen, Y. Dong, D. Saunders, A. Orock, E. Hodges, S. Colijn, N. Mamedova, R.A. Towner, OKN-007 Decreases

VEGFR-2 Levels in a Preclinical GL261 Mouse Glioma Model, Am. J. Nucl. Med. Mol. Imaging 5 (2015) 363-378.

[46] P.A. Aaron, M. Jamklang, J.P. Uhrig, A. Gelli, The Blood-Brain Barrier Internalises Cryptococcus Neoformans via the EphA2-Tyrosine Kinase Receptor, Cell. Microbiol. 20(3) (2018), https://doi.org/10.1111/cmi.12811.

[47] J.D. Ramsey, N.H. Flynn, Cell-Penetrating Peptides Transport Therapeutics into Cells, Pharmacol. Ther. 154 (2015) 78-86, https://doi.org/10.1016/j.pharmthera.2015.07.003.

[48] S.M. Farkhani, A. Valizadeh, H. Karami, S. Mohammadi, N. Sohrabi, F. Badrzadeh, Cell Penetrating Peptides: Efficient Vectors for Delivery of Nanoparticles, Nanocarriers, Therapeutic and Diagnostic Molecules, Peptides 57 (2014) 78-94, https://doi.org/10.1016/j.peptides.2014.04.015.

[49] D. Carradori, A.G. Dos Santos, J. Masquelier, A. Paquot, P. Saulnier, J. Eyer, V. Préat, G.G. Muccioli, M.P. Mingeot-Leclercq, A. des Rieux, The Origin of Neural Stem Cells Impacts Their Interactions with Targeted-Lipid Nanocapsules: Potential Role of Plasma Membrane Lipid Composition and Fluidity, J. Control. Release 292 (2018) 248-255, https://doi.org/10.1016/j.jconrel.2018.11.005.

[50] E. Moysan, G. Bastiat, J.P. Benoit, Gemcitabine versus Modified Gemcitabine: a review of several promising chemical modifications, Mol. Pharm. 10(2) (2013) 430-444. https://doi.org/10.1021/mp300370t.

[51] J.R. Kroep, W.J.P. Loves, C.L. van der Wilt, E. Alvarez, I. Talianidis, E. Boven, B.J.M. Braakhuis, C.J. van Groeningen, H.M. Pinedo, G.J. Peters, Pretreatment Deoxycytidine Kinase Levels Predict in Vivo Gemcitabine Sensitivity, Mol. Cancer Ther. 1(6) (2002) 371-376.

[52] K. Eder, B. Kalman, The dynamics of interactions among immune and glioblastoma cells, Neuromolecular Med. 17 (2015) 335-352, https://doi.org/10.1007/s12017-015-8362-x.

[53] D.F. Quail, J.A. Joyce, The microenvironmental landscape of brain tumors, Cancer Cell 31 (2017) 326-341, https://doi.org/10.1016/j.ccell.2017.02.009.

[54] E. Bozzato, N. Tsakiris, A. Paquot, G.G. Muccioli, C. Bastiancich, V. Préat, Dual-drug loaded nanomedicine hydrogel as a therapeutic platform to target both residual glioblastoma and glioma stem cells, Int. J. Pharm. 628 (2022) 122341, doi: 10.1016/j.ijpharm.2022.122341.